Inorg. Chem. **2005**, *44*, 770–778

Forum

X-ray Crystallography and Biological Metal Centers: Is Seeing Believing?

Monika Sommerhalter, Raquel L. Lieberman, and Amy C. Rosenzweig*

Department of Biochemistry, Molecular Biology, and Cell Biology and Department of Chemistry, Northwestern University, Evanston, Illinois 60208

Received October 20, 2004

Metalloenzyme crystal structures have a major impact on our understanding of biological metal centers. They are often the starting point for mechanistic and computational studies and inspire synthetic modeling chemistry. The strengths and limitations of X-ray crystallography in determining properties of biological metal centers and their corresponding ligand spheres are explored through examples, including ribonucleotide reductase R2 and particulate methane monooxygenase. Protein crystal structures locate metal ions within a protein fold and reveal the identities and coordination geometries of amino acid ligands. Data collection strategies that exploit the anomalous scattering effect of metal ions can establish metal ion identity. The quality of crystallographic data, particularly the resolution, determines the level of detail that can be extracted from a protein crystal structure. Complementary spectroscopic techniques can provide crucial information regarding the redox state of the metal center as well as the presence, type, and protonation state of exogenous ligands. The final result of the crystallographic characterization of a metalloenzyme is a model based on crystallographic data, supported by information from biophysical and modeling studies, influenced by sample handling, and interpreted carefully by the crystallographer.

Introduction

The unveiling of a new metalloenzyme crystal structure to the inorganic chemistry community typically generates great excitement accompanied by a multitude of questions regarding the metal center(s). Issues of importance include the locations, identities, stoichiometry, and redox states of the metal ions, the coordinated amino acids, the possible presence of exogenous ligands, and geometric parameters. These details then guide synthetic model preparation, computational studies, and mechanistic speculation. It is therefore crucial that inorganic chemists know whether to believe and how to interpret ball-and-stick or schematic diagrams of newly characterized metal centers. Some questions, such as metal ion location and identities of coordinating amino acid ligands, are answered best by crystallography. Whether and how well crystal structures elucidate features such as exogenous ligands and geometric parameters depends on the resolution, type, and quality of data, however. The higher the resolution, corresponding to a small value in angstroms (Å), the more detail can be seen for the metal center. Unlike small molecules, very few protein crystal structures are determined to atomic resolution. In addition, there is a component of interpretation by the macromolecular crystallographer, often aided by information from other techniques. In this Forum article, we explore the contribution of crystallography to defining the metal centers in the ribonucleotide reductase R2 subunit (R2) and particulate methane monooxygenase (pMMO), incorporating additional examples from our work and the literature to highlight specific points.

* To whom correspondence should be addressed. E-mail: amyr@northwestern.edu.

Metal Ion Identity and Stoichiometry

The first step in the characterization of a metalloenzyme is determining the metal ion content. This seemingly simple task can present a formidable challenge. The metal content of any protein sample can be determined by analytical methods such as inductively coupled plasma-atomic emission spectroscopy (ICP-AES) and atomic absorption spectroscopy (AAS), but the calculated stoichiometry also depends on how

10.1021/ic0485256 CCC: $30.25
Published on Web 01/28/2005

accurately the protein concentration is known. Often different methods of protein concentration determination, such as the Bradford assay,[1] the bicinchoninic acid (BCA) assay,[2] or use of the extinction coefficient at 280 nm, give different values. Another problem is that biological metal centers can be sensitive to the purification protocol employed. For example, metal centers can become depleted due to improper handling, air sensitivity, or inherent weak binding. In addition, adventitious metal ions might occupy both biologically relevant and nonspecific sites. Although careful biochemical and spectroscopic measurements can lead to accurate identities and stoichiometries, errors may influence subsequent spectroscopic and mechanistic characterization for years. Crystal structure determination plays a critical role in establishing both the identity and number of metal ions.

The ribonucleotide reductase R2 protein contains a carboxylate-bridged diiron center that generates a tyrosyl radical essential for production of deoxyribonucleotides by the associated R1 protein. There are numerous crystal structures of both prokaryotic and eukaryotic R2s.[3] Although now it is known that the dimeric R2 protein contains two dinuclear iron centers, totaling four iron ions, this stoichiometry was only firmly established by the first crystal structure, determined in 1990 to 2.2 Å resolution.[4] In 1969, the metal content for purified *E. coli* R2 was determined by a non-heme iron assay and wet combustion to be two irons per dimeric R2 molecule.[5] This quantity remained the status quo for nearly 20 years, and prior to the crystal structure, there was only one report of a stoichiometry closer to four.[3,6] Spectroscopic characterization[7−11] of R2 led to the generally accepted proposal that a single metal center composed of two high spin Fe(III) ions in an antiferromagnetically coupled binuclear, oxo-bridged complex was located at the dimer interface.[12] By contrast, the *E. coli* R2 crystal structure revealed two equivalent diiron centers, one in each monomer, separated by 25 Å.[4] The occupancy of these sites was estimated to be >85% by varying the occupancies of all four iron ions, conducting additional refinement cycles, and inspecting the resultant electron density maps[13] displaying the difference between the observed crystallographic data (F_o) and the model (F_c) ($F_o - F_c$ map).

The diiron centers of eukaryotic R2s are labile, and structures with the diiron clusters fully occupied have been difficult to obtain. In the 2.3 Å resolution structure of mouse R2, a single metal ion present in each active site was modeled as Fe(III) with an occupancy of 0.4.[14] The low metal occupancy in this structure may be attributable to the low pH buffer (pH 4.7) used for crystallization.[14] In support of this notion, soaking crystals of mouse R2 in a pH 6.0 buffer containing either Co(II)[15] or Fe(II)[16] resulted in the formation of dinuclear clusters. In our 3.1 Å resolution structure of the yeast R2 homodimer, also at a low pH, no metal ions are present in the active sites.[17] We did observe a partially occupied single metal site in our structure of the yeast R2 monomer in complex with the yeast Rnr4 protein,[18] a homologous protein that lacks an iron binding site, but is required for diiron cluster assembly in R2.[19]

Using data collected at wavelengths near the iron and zinc absorption edges, we modeled the metal ion in the yeast R2 monomer as adventitous Zn(II) instead of Fe(III).[18] It is possible that the mouse R2 metal site in the original structure actually contained Zn(II) as well. This approach, the collection and analysis of data at different wavelengths, is an important strategy for identifying metal ions and also for solving the phase problem for protein structures. Tunable synchrotron radiation sources allow data collection near the absorption edge of a specific metal ion. Absorption of radiation by the metal ion leads to anomalous scattering, a breakdown in Friedel's law.[20] This effect, detected in anomalous difference Fourier and Patterson maps, is exploited in the multiwavelength anomalous dispersion (MAD)[21,22] and single wavelength anomalous dispersion (SAD)[23] phasing techniques.

A crystal structure solved by copper MAD phasing and a relevant case study that sets the stage for a discussion of our work on pMMO is that of nitrous oxide reductase (N_2OR), an enzyme that reduces nitrous oxide to dinitrogen in the bacterial denitrification cycle.[24] Quantitation by ICP-AES and AAS indicated the presence of approximately four copper ions per N_2OR monomer. For a dozen years before

(1) Bradford, M. M. *Anal. Biochem.* **1976**, *72*, 248−254.
(2) Wiechelman, K. J.; Braun, R. D.; Fitzpatrick, J. D. *Anal. Biochem.* **1988**, *175*, 231−237.
(3) Eklund, H.; Uhlin, U.; Färnegårdh, M.; Logan, D. T.; Nordlund, P. *Prog. Biophys. Mol. Biol.* **2001**, *77*, 177−268.
(4) Nordlund, P.; Sjöberg, B.-M.; Eklund, H. *Nature* **1990**, *345*, 593−598.
(5) Brown, N. C.; Eliasson, R.; Reichard, P.; Thelander, L. *Eur. J. Biochem.* **1969**, *9*, 512−518.
(6) Lynch, J. B.; Juarez-Garcia, C.; Münck, E.; Que, L., Jr. *J. Am. Chem. Soc.* **1989**, *264*, 8091−8096.
(7) Atkin, C. L.; Thelander, L.; Reichard, P. *J. Biol. Chem.* **1973**, *248*, 7464−7472.
(8) Petersson, L.; Gräslund, A.; Ehrenberg, A. *J. Biol. Chem.* **1980**, *255*, 6706−6712.
(9) Bunker, G.; Petersson, L.; Sjöberg, B.-M.; Sahlin, M.; Chance, M.; Chance, B.; Ehrenberg, A. *Biochemistry* **1987**, *26*, 4708−4715.
(10) Scarrow, R. C.; Maroney, M. J.; Palmer, S. M.; Que, L., Jr.; Roe, L. A.; Salowe, S. P.; Stubbe, J. *J. Am. Chem. Soc.* **1987**, *109*, 7857−7864.
(11) Sjöberg, B.-M.; Loehr, T. M.; Sanders-Loehr, J. *Biochemistry* **1982**, *21*, 96−102.
(12) Thelander, L.; Reichard, P. *Annu. Rev. Biochem.* **1979**, *48*, 133−158.
(13) Nordlund, P.; Eklund, H. *J. Mol. Biol.* **1993**, *231*, 123−164.
(14) Kauppi, B.; Nielsen, B. B.; Ramaswamy, S.; Larsen, I. K.; Thelander, M.; Thelander, L.; Eklund, H. *J. Mol. Biol.* **1996**, *262*, 706−720.
(15) Strand, K. R.; Karlsen, S.; Andersson, K. K. *J. Biol. Chem.* **2002**, *277*, 34229−34238.
(16) Strand, K. R.; Karlsen, S.; Kolberg, M.; Røhr, Å. K. Gorbitz, C. H.; Andersson, K. K. *J. Biol. Chem.* **2004**, *279*, 46794−46801.
(17) Sommerhalter, M.; Voegtli, W. C.; Perlstein, D. L.; Ge, J.; Stubbe, J.; Rosenzweig, A. C. *Biochemistry* **2004**, *43*, 7736−7742.
(18) Voegtli, W. C.; Ge, J.; Perlstein, D. L.; Stubbe, J.; Rosenzweig, A. C. *Proc. Natl. Acad. Sci. U.S.A.* **2001**, *98*, 10073−10078.
(19) Ge, J.; Perlstein, D. L.; Nguyen, H. H.; Bar, G.; Griffin, R. G.; Stubbe, J. *Proc. Natl. Acad. Sci. U.S.A.* **2001**, *98*, 10067−10072.
(20) Stout, C. D.; Jensen, L. T. *X-ray structure determination: a practical guide*; John Wiley & Sons: New York, 1989.
(21) Hendrickson, W. A. *Science* **1991**, *254*, 51−58.
(22) Hendrickson, W. A.; Ogata, C. M. *Methods Enzymol.* **1997**, *276*, 494−523.
(23) Rice, L. M.; Earnest, T. N.; Brunger, A. T. *Acta Crystallogr., Sect. D* **2000**, *56*, 1413−1420.
(24) Zumft, W. G. *Microbiol. Mol. Biol. Rev.* **1997**, *61*, 533−616.

the first crystal structure determination in 2000,[25] these copper ions were postulated to be arranged in two dinuclear centers, a Cu_A electron transfer site and a catalytic center called Cu_Z.[26] The structure of the Cu_A site was correctly anticipated because it shares spectroscopic features and conserved copper ligands with the cytochrome *c* oxidase Cu_A site. The details of the Cu_A-type center had in fact eluded the bioinorganic community for almost 40 years, but Cu_A was well characterized[27] prior to the N_2OR structure determination. By contrast, the Cu_Z site revealed by the 2.4 Å resolution structure of *Pseudomonas nautica* N_2OR[25] was a complete surprise, containing four copper ions instead of the expected two, giving a stoichiometry of six rather than four copper ions per monomer. The 9−12 copper ions measured per *P. nautica* N_2OR dimer[28] is consistent with this stoichiometry, and lower values obtained for N_2OR from other organisms could be due to an overestimation of the protein concentration[28] or copper loss during purification. How did the crystallographers know that there were four copper ions in the Cu_Z site? At 2.4 Å resolution, with Cu···Cu distances of ∼2.5−3 Å,[25] the four copper ions may have been just distinguishable in the electron density map. The tetranuclear site was initially modeled by successively introducing individual copper ions into positive peaks in the $F_o - F_c$ map followed by iterative cycles of refinement.[25] Further confirmation of the tetranuclear cluster came from the 1.6 Å resolution structure of *Paracoccus denitrificans* N_2OR (Figure 1).[29,30]

We recently determined the first crystal structure of another copper-containing metalloenzyme, pMMO from *Methylococcus capsulatus* (Bath).[31] pMMO is an integral membrane enzyme that oxidizes methane to methanol in methanotrophic bacteria.[32,33] Crystallization was challenging because integral membrane proteins have limited hydrophilic or polar surfaces to make good crystal contacts. Instead, surface residues are primarily hydrophobic in order to interact with the surrounding lipid bilayer. Nevertheless, crystals can be obtained in the presence of detergents.[34] We determined the structure to 2.8 Å resolution, excellent for a membrane protein, but significantly lower than that of the R2 and N_2OR structures. Structures of other membrane-bound metalloenzymes such as cytochrome *c* oxidase[35,36] and photosystem II[37] have also been determined to medium resolution. Unlike R2 and N_2OR, there has been little convergence in the literature about the metal ion content of pMMO over the past 10 years. For each ∼100 kDa pMMO monomer composed of three subunits (pmoB or α, ∼47 kDa; pmoA or β, ∼24 kDa; pmoC or γ, ∼22 kDa), ranges of 2−15 copper ions and 0−2.5 iron ions have been reported.[32] The variation in metal ion content may be due to differing protocols for isolating the membrane fractions and/or measuring the protein concentration.[32,38]

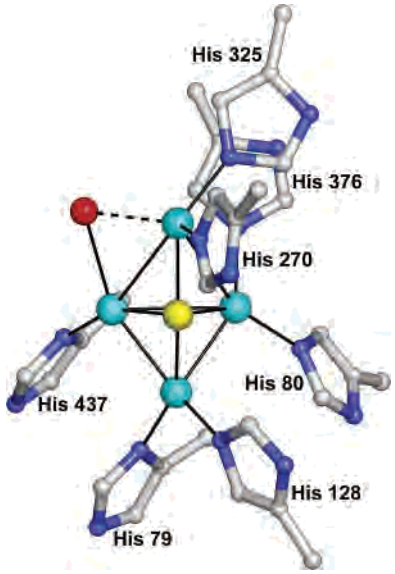

Figure 1. The tetranuclear Cu_Z site in the 1.6 Å resolution structure of *P. denitrificans* N_2OR (PDB accession code 1FWX). The copper ions are shown as cyan spheres, a solvent molecule is shown as a red sphere, and a bridging sulfur atom is shown as a yellow sphere.

Several research groups have proposed models for the pMMO metal center(s). On the basis of the hyperfine splitting pattern of an isotropic electron paramagnetic resonance (EPR) signal at $g = 2.06$, Chan and co-workers propose that pMMO contains 5−7 mixed valence trinuclear copper clusters, of which some function in catalysis and some function in electron transfer.[39,40] By contrast, Dispirito and co-workers have suggested the presence of both copper and iron sites, perhaps in a mixed metal cluster. In their model, additional copper is associated with pMMO as part of a small copper binding compound called methanobactin.[41−43] Finally, our EPR and X-ray absorption spectroscopic data are

(25) Brown, K.; Tegoni, M.; Prudêncio, M.; Pereira, A. S.; Besson, S.; Moura, J. J.; Moura, I.; Cambilleau, C. *Nat. Struct. Biol.* **2000**, *7*, 191−195.
(26) Rosenzweig, A. C. *Nat. Struct. Biol.* **2000**, *7*, 169−171.
(27) Beinert, H. *Eur. J. Biochem.* **1997**, *245*, 521−532.
(28) Prudêncio, M.; Pereira, A. S.; Tavares, P.; Besson, S.; Cabrito, I.; Brown, K.; Samyn, B.; Devreese, B.; Beeumen, J. V.; Rusnak, F.; Fauque, G.; Moura, J. J. G.; Tegoni, M.; Cambillau, C.; Moura, I. *Biochemistry* **2000**, *39*, 3899−3907.
(29) Brown, K. R.; Djinovic-Carugo, K.; Haltia, T.; Cabrito, I.; Saraste, M.; Moura, J. J. G.; Moura, I.; Tegoni, M.; Cambillau, C. *J. Biol. Chem.* **2000**, *275*, 41133−41136.
(30) Haltia, T.; Brown, K.; Tegoni, M.; Cambillau, C.; Saraste, M.; Matilla, K.; Djinovic-Carugo, K. *Biochem. J.* **2003**, *369*, 77−88.
(31) Lieberman, R. L.; Rosenzweig, A. C. *Nature* advance online publication, Jan 26, 2005 (doi: 10.1038/nature03311).
(32) Lieberman, R. L.; Rosenzweig, A. C. *Crit. Rev. Biochem. Mol. Biol.* **2004**, *39*, 147−164.
(33) Chan, S. I.; Chen, K. H.-C.; Yu, S. S.-F.; Chen, C.-L.; Kuo, S. S.-J. *Biochemistry* **2004**, *43*, 4421−4430.
(34) Kühlbrandt, W. *Q. Rev. Biophys.* **1988**, *21*, 429−477.
(35) Tsukihara, T.; Aoyama, H.; Yamashita, E.; Tomizaki, T.; Yamaguchi, H.; Shinzawa-Itoh, K.; Nakashima, R.; Yaono, R.; Yoshikawa, S. *Science* **1995**, *269*, 1069−1074.
(36) Iwata, S.; Ostermeier, C.; Ludwig, B.; Michel, H. *Nature* **1995**, *376*, 660−669.
(37) Ferreira, K. N.; Iverson, T. M.; Maghloaoui, K.; Barber, J.; Iwata, S. *Science* **2004**, *303*, 1831−1838.
(38) Lieberman, R. L.; Shrestha, D. B.; Doan, P. E.; Hoffman, B. M.; Stemmler, T. L.; Rosenzweig, A. C. *Proc. Natl. Acad. Sci. U.S.A.* **2003**, *100*, 3820−3825.
(39) Nguyen, H.-H. T.; Shiemke, A. K.; Jacobs, S. J.; Hales, B. J.; Lidstrom, M. E.; Chan, S. I. *J. Biol. Chem.* **1994**, *269*, 14995−15005.
(40) Nguyen, H.-H. T.; Nakagawa, K. H.; Hedman, B.; Elliott, S. J.; Lidstrom, M. E.; Hodgson, K. O.; Chan, S. I. *J. Am. Chem. Soc.* **1996**, *118*, 12766−12776.
(41) Zahn, J. A.; DiSpirito, A. A. *J. Bacteriol.* **1996**, *178*, 1018−1029.
(42) Choi, D. W.; Kunz, R. C.; Boyd, E. S.; Semrau, J. D.; Antholine, W. E.; Han, J. I.; Zahn, J. A.; Boyd, J. M.; de la Mora, A. M.; DiSpirito, A. A. *J. Bacteriol.* **2003**, *185*, 5755−5764.

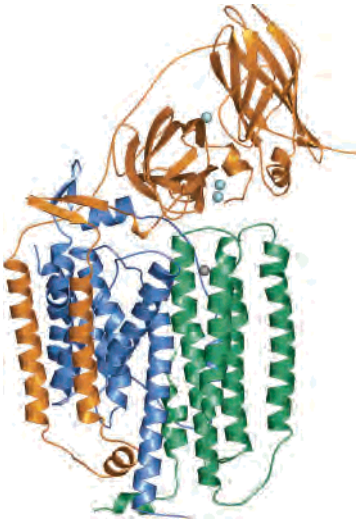

Figure 2. One protomer from the *M. capsulatus* (Bath) pMMO trimer (PDB accession code 1YEW). The protomer comprises one copy each of three subunits, pmoA (blue), pmoB (orange), and pmoC (green). A mononuclear and a dinuclear copper site (cyan spheres) are located in the soluble regions of the pmoB subunit, and a zinc site (gray sphere) is located within the membrane between the pmoA and pmoC subunits.

consistent with a mononuclear, type 2 Cu(II) center ligated by histidine residues and a copper-containing cluster characterized by a 2.57 Å Cu−Cu interaction. Since we typically measure ∼1 Fe ion per monomer by ICP-AES, a functional iron center could also be present.[32,38]

Like N_2OR, we were able use the knowledge that pMMO contains copper to solve the structure. We obtained phases by copper SAD and improved them by noncrystallographic symmetry averaging.[23] Using anomalous data collected at an energy of 9004 eV, we located six copper sites arranged in pairs around a 3-fold axis, indicating for the first time that pMMO is a trimer. Additional metal ions observed in the electron density map were identified as zinc by analysis of anomalous data collected at 9686 eV, near the zinc absorption edge. We know that these metal ions are not copper because they are not evident in anomalous maps calculated from data collected near the copper edge, which is lower in energy than the zinc edge. There is one zinc site within pMMO as well as several zinc ions at crystal contacts. Finally, we collected multiple data sets at the iron edge, but the absence of significant peaks in resulting anomalous maps led us to conclude that there is no iron in the crystals. Thus, each protomer in our crystal structure contains two distinct copper sites and a zinc site (Figure 2). These findings are consistent with values of 2−3 copper ions per 100 kDa,[38,44] but in conflict with other reported stoichiometries of 12−15 copper ions.[45,46]

Our structure does not allow for unambiguous assignment of the nuclearity of the copper sites since extended X-ray absorption fine structure (EXAFS) data indicate a Cu···Cu distance of 2.57 Å,[38] shorter than the 2.8 Å maximum resolution of the data. We have interpreted the data as one mononuclear (Figure 3a) and one dinuclear (Figure 3b) site. Assignment of the dinuclear site was based on two observations. First, the peak in the 3.0 Å resolution anomalous electron density map generated from data collected at the copper absorption edge has an oblong shape. Second, the 2.8 Å resolution anomalous map calculated using data collected at the zinc edge exhibits two peaks, 2.6 Å apart, at this site (Figure 3b). This distance is consistent with our EXAFS result. The same anomalous map calculated to 3.0 Å resolution only shows a single peak, underscoring the importance of resolution. Since the zinc edge is higher in energy than the copper edge, we observe an anomalous signal due to copper at this wavelength also. The second site was modeled as a mononuclear center since we have no evidence to suggest there is more than one copper ion present (Figure 3a). For both sites, inclusion of additional copper ions led to significant negative $F_o - F_c$ density, indicating that a trinuclear copper cluster is not present. We attempted to correlate nuclearity with anomalous peak heights as well. In the 2.8 Å resolution crystal structure of bovine heart cytochrome *c* oxidase, which contains a dinuclear Cu_A site and a mononuclear Cu_B site, the order of peak heights in an anomalous map was consistent with the nuclearity of each site.[35] This type of analysis was inconclusive for pMMO, however. We also note that the cytochrome *c* oxidase case was far more straightforward because the nuclearity of Cu_A had been established by EPR spectroscopy prior to the crystal structure determination.[27]

The presence of a mononuclear zinc site (Figure 3c) in pMMO is intriguing. Our ICP-AES measurements indicate there is no Zn(II) associated with purified pMMO so the Zn(II) ions likely derive from the crystallization buffer.[31] It is not clear, however, whether the site is adventitious or is ordinarily occupied by another metal ion. There are numerous examples of Zn(II) replacing a physiologically relevant metal ion, although it is more typical for Zn(II) to copurify with the protein than to bind during crystallization. In addition to our yeast R2 structure[18] (vide supra), Zn(II) was found in the type 1 Cu(I) electron transfer site of a nitrite reductase mutant.[47] A variety of metal ions have also been identified in structures of carbon monoxide dehydrogenase/acetyl CoA synthase (CODH/ACS). In structures obtained by different investigators, the dinuclear A cluster in acetyl CoA synthase contains two nickel ions,[48] nickel and zinc,[49] or nickel and copper.[50] These different combinations of metal ions were assigned on the basis of careful analysis of anomalous data.

(43) Kim, H. J.; Graham, D. W.; DiSpirito, A. A.; Alterman, M. A.; Galeva, N.; Larive, C. K.; Asunskis, D.; Sherwood, P. M. A. *Science* **2004**, *305*, 1612−1615.
(44) Basu, P.; Katterle, B.; Andersson, K. K.; Dalton, H. *Biochem. J.* **2003**, *369*, 417−427.
(45) Nguyen, H. H.; Elliott, S. J.; Yip, J. H.; Chan, S. I. *J. Biol. Chem.* **1998**, *273*, 7957−7966.
(46) Yu, S. S.-F.; Chen, K. H.-C.; Tseng, M. Y.-H.; Wang, Y.-S.; Tseng, C.-F.; Chen, Y.-J.; Huang, D. S.; Chan, S. I. *J. Bacteriol.* **2003**, *185*, 5915−5924.
(47) Murphy, M. E. P.; Turley, S.; Kukimoto, M.; Nishiyama, M.; Horinouchi, S.; Sasaki, H.; Tanokura, M.; Adman, E. T. *Biochemistry* **1995**, *34*, 12107−12117.
(48) Darnault, C.; Volbeda, A.; Kim, E. J.; Legrand, P.; Vernède, X.; Lindahl, P. A.; Fontecilla-Camps, J. C. *Nat. Struct. Biol.* **2003**, *10*, 271−279.
(49) Svetlitchnyi, V.; Dobbek, H.; Meyer-Klaucke, W.; Meins, T.; Thiele, B.; Römer, P.; Huber, R.; Meyer, O. *Proc. Natl. Acad. Sci. U.S.A.* **2004**, *101*, 446−451.

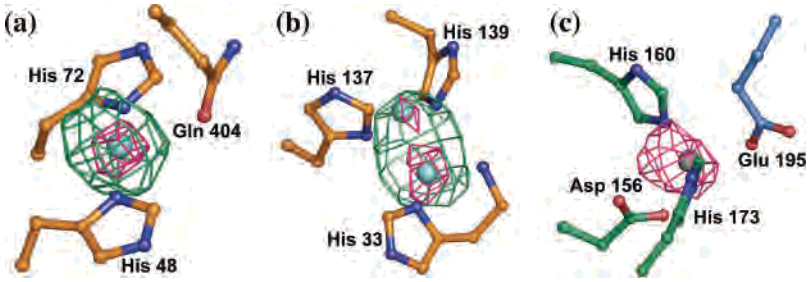

Figure 3. Metal sites in the 2.8 Å resolution pMMO structure. The anomalous difference Fourier electron density maps for data collected near the copper absorption edge (green, 3 Å resolution) and near the zinc absorption edge (magenta, 2.8 Å resolution) are superimposed. Both maps are contoured at 4σ. (a) The mononuclear copper site. (b) The dinuclear copper site. All ligands for the copper sites are derived from pmoB (orange carbon atoms). (c) The zinc site. The zinc ion is coordinated by residues from both pmoC (green carbon atoms) and pmoA (blue carbon atoms).

The dinickel form is believed to be physiologically relevant.[51] It is possible that the Zn(II) site in pMMO binds copper or iron in vivo, but further experiments, including crystallization in the absence of zinc, are warranted.

In sum, metalloenzyme crystal structures can provide critical information regarding the identity and stoichiometry of bound metal ions. Identification of metal ions requires collection of anomalous data at appropriate energies. Without such data, commonly found metal ions such as iron, copper, and zinc cannot be distinguished. Stoichiometries determined from crystal structures often differ significantly from those measured for the purified protein by analytical techniques. In the event that metal ions are closer together than the resolution of the structure, establishing nuclearity can present a problem. Finally, nonphysiological metal ions can occupy metal binding sites, and other techniques are required to determine the composition of the active form.

Redox States of Metal Ions

To use crystal structures of metalloenzyme active sites as starting points for mechanistic schemes or computational analysis, knowledge of the metal oxidation state is required. It is not possible to determine oxidation state with absolute certainty from a crystal structure. Typically, redox state is assumed on the basis of characterization of the sample used for crystallization, inferred from the observed coordination environment, or in the best cases, determined by single crystal microspectrophotometry.[52] The R2 crystals used for the initial structure determination were shown by optical spectroscopy to contain a diiron(III) center.[13] A single crystal optical spectrum was also reported for N_2OR.[25] This spectrum exhibited characteristics of the reduced "blue" form of the enzyme in which Cu_A is dicopper(I) and Cu_Z is proposed to comprise one Cu(II) and three Cu(I) ions. Which of the four copper ions is Cu(II) cannot be determined directly from the crystal structure, but density functional theory (DFT) calculations have indicated partial delocalization with the copper ion coordinated by His 270 and His 325 (Figure 1) dominantly oxidized.[53] The oxidation states of the copper ions in the pMMO structure are unknown, although a crude single crystal X-ray absorption scan indicates the presence of Cu(I). According to EPR and X-ray absorption spectroscopic data, purified pMMO contains ~30−60% Cu(II).[32] Therefore, the crystals likely contain a mixture of Cu(I) and Cu(II). pMMO does not exhibit any redox dependent optical spectroscopic features, but single crystal EPR or EXAFS might provide some insight into the oxidation state.

Another important issue regarding redox state is the phenomenon of photoreduction in the X-ray beam. Some crystals undergo a change in oxidation state during data collection. For example, both the ferric and compound III forms of horseradish peroxidase become reduced at an X-ray dose far less than that required to complete a data set. This finding, particularly relevant to structural characterization of short-lived catalytic intermediates, also has scary implications for metalloprotein structures in general.[54] Many crystallographically characterized metal centers may actually represent mixtures of redox states. Photoreduction can also prove advantageous. The 1.7 Å resolution of reduced *E. coli* R2 was obtained fortuitously by thawing and refreezing oxidized crystals after exposure to synchrotron radiation (Figure 4b). This structure is the same as that obtained by chemically reducing R2 crystals with dithionite and phenosafranin.[55] For *Salmonella typhimurium* R2[56] and a related diiron enzyme, stearoyl acyl carrier protein Δ^9 desaturase,[57] photoreduction occurred without thawing and refreezing the crystal. Both the *E. coli* and *S. typhimurium* R2 crystals only photoreduced in the presence of glycerol, which is a good electron hole stabilizer.[55,56] This result could have broader implications, considering that glycerol is widely used as a cryoprotectant.

Once a structure is obtained in some defined or assumed redox state, it is possible to alter this state in the crystal. For example, crystals of apo or oxidized protein can be reduced by several methods. First, crystals of apo protein can be soaked in a solution containing metal ions of the desired

(50) Doukov, T. I.; Iverson, T. M.; Seravalli, J.; Ragsdale, S. W.; Drennan, C. L. *Science* **2002**, *298*, 567−572.
(51) Drennan, C. L.; Doukov, T. I.; Ragsdale, S. W. *J. Biol. Inorg. Chem.* **2004**, *9*, 511−515.
(52) Wilmot, C. M.; Sjögren, T.; Carlsson, G. H.; Berglund, G. I.; Hadju, J. *Methods Enzymol.* **2002**, *353*, 301−318.
(53) Chen, P.; DeBeer, G., S.; Cabrito, I.; Antholine, W. E.; Moura, J. J. G.; Moura, I.; Hedman, B.; Hodgson, K. O.; Solomon, E. I. *J. Am. Chem. Soc.* **2002**, *124*, 744−745.
(54) Berglund, G. I.; Carlsson, G. H.; Smith, A. T.; Szöke, H.; Henriksen, A.; Hajdu, J. *Nature* **2002**, *417*, 463−468.
(55) Logan, D. T.; Su, X.-D.; Åberg, A.; Regnström, K.; Hajdu, J.; Eklund, H.; Nordlund, P. *Structure* **1996**, *4*, 1053−1064.
(56) Eriksson, M.; Jordan, A.; Eklund, H. *Biochemistry* **1998**, *37*, 13359−13369.
(57) Lindqvist, Y.; Huang, W.; Schneider, G.; Shanklin, J. *EMBO J.* **1996**, *15*, 4081−4092.

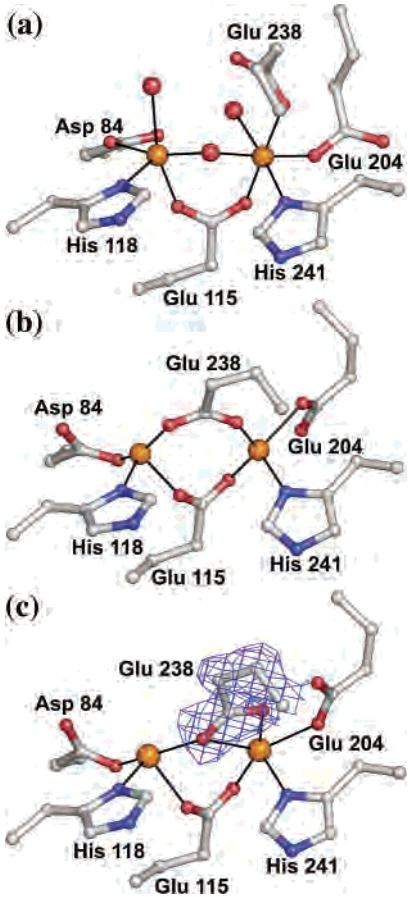

Figure 4. The diiron center in *E. coli* R2. The iron ions are shown as orange spheres, and exogenous oxygen ligands are shown as red spheres. (a) The oxidized diiron(III) form determined to 1.4 Å resolution (PDB accession code 1MXR). (b) The photoreduced diiron(II) form (PDB accession code 1XIK). (c) The ferrous soaked diiron(II) form (PDB accession code 1PIY). A simulated annealing omit map for Glu 238 is superimposed (contoured at 4.5σ, blue). Both reduced structures were determined to 1.7 Å resolution.

oxidation state prior to freezing. Second, reductants such as dithionite or ascorbate, sometimes in combination with organic mediator compounds such as methyl viologen or phenosafranin, can be added to crystals. Third, the protein solution can be reduced, reductants removed by dialysis or column chromatography, crystals grown in an anaerobic box, and frozen in a reduced or degassed cryoprotecant solution. The fourth option is photoreduction, as described above. For all these methods, verification of redox state presents a problem. In the simplest cases, visual inspection of the crystal suffices. We were able to reduce nitrosocyanin, a red copper protein from *Nitrosomonas europaea*, with dithionite, yielding a colorless solution. Crystals of this reduced, colorless form were then obtained under anaerobic conditions.[58] In many cases, reduction is deemed successful if changes in coordination consistent with the desired oxidation state are observed. It should be noted, however, that assigning oxidation state solely based on metal−ligand distances is usually not possible unless very high resolution data are available.

Even if a reduced structure is obtained and verified, there is no guarantee that it represents the reduced structure in solution. Crystallization conditions, particularly pH, and crystal packing effects may influence the resulting structure. In addition, the reduction procedure itself can affect the outcome. We have prepared crystals of diiron(II) *E. coli* R2 both by chemical reduction of oxidized crystals and by soaking apo crystals in solutions of Fe(II).[59] Suprisingly, two different coordination geometries result from the two procedures (Figure 4b,c). The structures of the "ferrous soaked" forms are more consistent with circular dichroism (CD) and magnetic circular dichroism (MCD) spectroscopic data (vide infra).

Overall, redox state is difficult to ascertain solely from crystal structures, and many structures might represent mixtures of redox states. Single crystal optical, EPR, and X-ray absorption spectroscopic analysis can be highly beneficial, but are not trivial, and require an experienced spectroscopic collaborator and sometimes more or larger crystals than are readily available. Complications due to photoreduction and varying procedures for generating reduced states in crystals can occur as well. Finally, there is no guarantee that any structure of any oxidation state is mechanistically relevant. Mechanistic relevance can be ascertained by conducting activity assays on crystals or obtaining cocrystal structures with substrates or inhibitors. These caveats should be kept in mind when using such structures as starting models for mechanistic speculation and computational studies.

Protein Ligand Identity and Coordination Geometry

Unlike redox state, the identities of amino acid ligands are discerned readily from metalloenzyme crystal structures. Whereas spectroscopic analysis can indicate ligand type, e.g., oxygen or nitrogen, or provide estimates of coordination number, crystallography yields a detailed picture of the metal center within the protein environment. Site-directed mutagenesis, sequence alignments, and homology modeling can suggest the involvement of specific residues, but direct evidence can only be obtained from the structure. For high resolution structures, not only can amino acid ligands be identified, but also coordination distances and geometry can be determined. All of the *E. coli* R2 structures have been determined to 2.5 Å resolution or better.[3] The diiron center is housed within a four helix bundle with the two iron ions coordinated by two histidine residues, His 118 and His 204, one aspartic acid, Asp 84, and three glutamic acid residues, Glu 115, Glu 204, and Glu 238 (Figure 4).[4] These residues are highly conserved in R2 proteins from other species.[3] One exception is the yeast Rnr4 protein which contains two tyrosines in place of the histidines and an arginine instead of one of the glutamic acid residues. Not surprisingly, this protein does not bind iron.[18,19]

In all the R2 structures, each iron ion is coordinated by the δ nitrogen atom of a histidine residue and residue Glu

(58) Lieberman, R. L.; Arciero, D. M.; Hooper, A. B.; Rosenzweig, A. C. *Biochemistry* **2001**, *40*, 5674−5681.

(59) Voegtli, W. C.; Sommerhalter, M.; Saleh, L.; Baldwin, J.; Bollinger, J. M., Jr.; Rosenzweig, A. C. *J. Am. Chem. Soc.* **2003**, *125*, 15822−15830.

115 bridges the two iron ions in a μ-1,3 fashion. The coordination modes of the other three carboxylate ligands vary and are not so clear in some cases. How accurately the binding mode of these residues is described depends on several factors, including the resolution. On the basis of the original 2.2 Å resolution structure of oxidized *E.coli* R2, Asp 84 was described as bidentate to Fe1 (Fe−O distances of 2.4 and 2.5 Å).[13,60] This residue was later assigned as monodentate in the 1.4 Å resolution structure (Fe−O distances of 2.0 and 2.9 Å) (Figure 4a).[61] Notably, computational studies support a monodentate binding mode for Asp 84.[62] A related factor influencing how the carboxylate binding modes are assigned is the coordinate error. The coordinate error can be estimated by different methods, including the Luzzati plot,[63] the σ_A plot,[64] or the Cruickshank diffraction-component precision index (DPI).[65] Even for the 1.4 Å resolution R2 structure, the coordinate error is approximately 0.1 Å. Therefore, the crystallographer often makes a subjective decision on whether to depict a ligand as coordinating.

Coordination geometry inferred from a crystal structure does not always agree with spectroscopic data. The initial reduced R2 structure with both Fe(II) ions four-coordinate[55] (Figure 4b) is inconsistent with CD and MCD spectra indicating the presence of one four-coordinate and one five-coordinate Fe(II).[66] Which description is correct? One possibility is that the solution form of the protein used for spectroscopy has a different diiron(II) center than that observed in the crystals used for the original structure.[55] Our recent structures of the "ferrous soaked" form of R2 support this explanation.[59] Whereas Glu 238 bridges the two iron ions in a μ-1,3 fashion after chemical or photoreduction at pH 5−6 (Figure 4b), soaking apo R2 crystals in Fe(II) at both pH 5 and pH 7 results in μ-(η^1,η^2) coordination. This geometry is quite clear from an $F_o - F_c$ map calculated after omitting Glu 238 from the refinement (Figure 4c), and was observed consistently in multiple crystals. The μ-(η^1,η^2) coordination of Glu 238, also observed in several R2 variants,[67−69] renders Fe2 five-coordinate and suggests that this structure may correspond to the species present in the CD/MCD samples. Similarly, structures of the ferrous soaked R2-D84E and R2-D84E/W48F mutants are more compatible with CD/MCD data.[59,70] Computational studies indicate that the two coordination modes of Glu 238 are close in energy,[62,70] consistent with the observation of both in structures of reduced R2. This example underscores the possibility that a metal center observed in a structure may be affected by the crystal preparation method and may not represent that in solution. This is particularly important for the R2 case since the original diiron(II) structure (Figure 4b) has been widely used as a starting model for studying the O_2 activation mechanism.

Sometimes multiple views of the same metal center are available in a single crystal structure. *E. coli* R2 crystallizes with a dimer in the asymmetric unit, and the two halves of the dimer are treated individually in the crystallographic refinement. In the photoreduced diiron(II) structure (Figure 4b), the distances between the two oxygen atoms of Glu 204 and the iron ions vary, with distances of 2.17 and 2.88 Å in monomer A and 2.44 and 2.50 Å in monomer B.[55] Thus, Glu 204 is clearly terminal monodentate in monomer A but could be assigned as bidentate with somewhat long coordination distances in monomer B. Taking the coordinate error into account, 2.44 and 2.50 Å could also be consistent with monodentate, terminal ligation. Since the electron density was better defined in monomer A, the monodentate model was chosen. Discrepancies between the two halves of the dimer are actually quite common in the array of *E. coli* R2 structures. Another way of acquiring independent views of a metal center is to obtain a new crystal form using different crystallization conditions. Although not always possible, such a comparison can establish whether crystal lattice contacts or components of the crystallization buffer affect the observed coordination geometry.

In contrast to the wealth of information regarding the ligand sphere of the R2 diiron center, knowledge of the pMMO metal centers is in its infancy. The major findings from our 2.8 Å resolution crystal structure include the location of the metal centers and the identities of the protein ligands. As described above, three distinct metal centers have been modeled: a mononuclear copper site, a dinuclear copper site, and a mononuclear zinc site, which likely houses a different metal ion in vivo. The two copper sites are located ∼21 Å apart in the soluble region of the pmoB subunit (Figure 2). The mononuclear center is ∼25 Å above the membrane whereas the dinuclear site is closer to the interface between the soluble and membrane-bound regions. The zinc site is located ∼10 Å below the membrane surface primarily within pmoC (Figure 2). According to radiolabeling studies with the suicide substrate acetylene, the pMMO active site was predicted to reside on pmoA, with some involvement of pmoB.[41,71] Although the active site has not been identified, pmoA does not house either copper site and only provides one ligand to the zinc site.

At 2.8 Å resolution, coordinating residues can be identified from the electron density, but the high coordinate error precludes quoting meaningful bond distances. The copper ion in the mononuclear site is coordinated by His 48 and His 72. A glutamine, Gln 404, is also within ∼3 Å of the

(60) Nordlund, P. Ph.D. Thesis, Swedish University of Agricultural Sciences, 1990.
(61) Högbom, M.; Galander, M.; Andersson, M.; Kolberg, M.; Hofbauer, W.; Lassmann, G.; Nordlund, P.; Lendzian, F. *Proc. Natl. Acad. Sci. U.S.A.* **2003**, *100*, 3209−3214.
(62) Torrent, M.; Musaev, D. G.; Morokuma, K. *J. Phys. Chem. B* **2001**, *105*, 322−327.
(63) Luzatti, P. V. *Acta Crystallogr.* **1952**, *5*, 802−810.
(64) Read, R. J. *Acta Crystallogr.* **1986**, *A42*, 140−149.
(65) Cruickshank, D. W. J. *Acta Crystallogr.* **1999**, *D55*, 583−601.
(66) Pulver, S. C.; Tong, W. H.; Bollinger, J. M., Jr.; Stubbe, J.; Solomon, E. I. *J. Am. Chem. Soc.* **1995**, *117*, 12664−12678.
(67) Andersson, M. E.; Högbom, M.; Rinaldo-Matthis, A.; Andersson, K. K.; Sjöberg, B.-M.; Nordlund, P. *J. Am. Chem. Soc.* **1999**, *121*, 2346−2352.
(68) Voegtli, W. C.; Khidekel, N.; Baldwin, J.; Ley, B. A.; Bollinger, J. M., Jr.; Rosenzweig, A. C. *J. Am. Chem. Soc.* **2000**, *122*, 3255−3261.
(69) Högbom, M.; Andersson, M. E.; Nordlund, P. *J. Biol. Inorg. Chem.* **2001**, *6*, 315−323.
(70) Wei, P.-P.; Skulan, A. J.; Mitic, N.; Yang, Y.-S.; Saleh, L.; Bollinger, J. M., Jr.; Solomon, E. I. *J. Am. Chem. Soc.* **2004**, *126*, 3777−3788.
(71) Cook, S. A.; Shiemke, A. K. *J. Inorg. Biochem.* **1996**, *63*, 273−284.

copper ion (Figure 3a). Interestingly, His 72 is not conserved among pMMOs from other organisms, appearing most often as an asparagine. Both the *M. capsulatus* (Bath) gene sequences originally reported[72] and those from the complete genome[73] contain a histidine at this position, however. Three conserved histidines provide ligands to the dinuclear site, His 33, His 137, and His 139. The amino nitrogen of His 33, which corresponds to the N-terminus of pmoB, is also within coordinating distance of one of the copper ions (Figure 3b). The zinc ion is coordinated by four highly conserved residues, Asp 156, His 160, and His 173 from pmoC and Glu 195 from pmoA (Figure 3c). It should be noted that the three protomers in the pMMO trimer were refined using noncrystallographic symmetry restraints, a strategy appropriate for a 2.8 Å resolution structure.[74] Therefore, the trimer does not provide three independent views of the metal centers.

In general, there is no substitute for a crystal structure for placing metal centers within the overall fold of a protein and for identifying amino acid ligands. The determination of metrical parameters depends critically on resolution, however. Comparisons of multiple structures coupled with information from spectroscopy and calculations can help resolve ambiguities regarding coordination number and geometry.

Exogenous Ligands

An important feature of many biological metal centers is the presence of exogenous ligands. These nonprotein ligands cannot be inferred from the amino acid sequence of the protein and must either be discovered in the electron density map or known to be part of the active site through other methods. Clear identification of the type and coordination geometry of an exogenous ligand requires a combination of crystallographic, spectroscopic, and biochemical data. The diiron(III) form of R2 contains three exogenous ligands: a μ-oxo (O^{2-}) bridge and one water molecule coordinated terminally to each iron ion (Figure 4a). The nature of the bridging exogenous ligands in both R2 and a similar diiron enzyme, the soluble methane monooxygenase hydroxylase (MMOH), were established by spectroscopy[75] prior to the crystal structures. Although the coordination spheres in the two proteins only differ in the replacement of R2 Asp 84 with a glutamic acid in MMOH, oxidized MMOH contains a μ-hydroxo, rather than a μ-oxo, group. In particular, proton electron nuclear double resonance (ENDOR) studies played a key role in establishing the presence of a bridging hydroxide in MMOH.[76] At 2.2 Å resolution, the resolution of the original R2[60] and MMOH[77] structures, hydrogen atoms cannot be distinguished. Only structures to better than 1 Å resolution, often referred to as ultrahigh resolution, provide information regarding hydrogen atoms. The number of such structures, while increasing,[78] remains limited for metalloproteins. Therefore, spectroscopic data facilitated assignment of these bridging ligands in the electron density maps. Correctly placing these bridging solvent ligands was also challenging since the metal to ligand distance is less than 2.2 Å. For example, the position of the μ-oxo bridge in R2 was dependent on the iron occupancies used in the refinement.[13]

In addition to coordinating metal ions, solvent molecules often play important roles in stabilizing active sites by hydrogen bonding to ligating residues or participating in a reaction mechanism. Whether water molecules are included in a structure and how many are modeled depends on the resolution. Roughly one water molecule per protein residue is typically modeled at ~2 Å resolution whereas no water molecules are likely to be discerned at ~3 Å resolution.[79] Criteria used in assigning water molecules include significant electron density, reasonable temperature factors, and the presence of obvious hydrogen bonding partners. Notably, theoretical optimization of the reduced MMOH structure led to the discovery of a previously unidentified water molecule in the electron density map.[80] For our 2.8 Å resolution pMMO structure, no water molecules were modeled. It is quite likely, however, that one or both of the copper centers contain exogenous ligands. In particular, the dinuclear site may have bridging ligands that we have not yet identified.

The N_2OR structure is instructive in considering what additional ligands may be present in pMMO. In the 2.4 Å resolution *P. nautica* N_2OR structure, a water or hydroxide ligand was modeled capping the four copper ions.[25] This model was difficult to reconcile with spectroscopic data suggesting sulfur ligation, however.[81] Subsequent elemental analysis coupled with resonance Raman spectroscopy led to the proposal that this ligand is actually inorganic sulfide, not oxygen.[82] Shortly thereafter, the presence of sulfide was confirmed by the 1.6 Å resolution crystal structure of *P. denitrificans* N_2OR and a re-examination of the *P. nautica* structure[29] (Figure 1). The peak height for the bridging sulfide in the 1.6 Å resolution electron density map was comparable to that observed for other sulfur atoms, such as those derived from methionine, rather than to density attributable to oxygen. Re-refinement of *P. nautica* Cu_Z with sulfide led to

(72) Semrau, J. D.; Chistoserdov, A.; Lebron, J.; Costello, A.; Davagnino, J.; Kenna, E.; Holmes, A. J.; Finch, R.; Murrell, J. C.; Lidstrom, M. E. *J. Bacteriol.* **1995**, *177*, 3071−3079.
(73) Ward, N.; Larsen, O.; Sakwa, J.; Bruseth, L.; Khouri, H.; Durkin, A. S.; Dimitrov, G.; Jiang, L.; Scanlan, D.; Kang, K. H.; Lewis, M.; Nelson, K. E.; Metheacute, B.; Wu, M.; Heidelberg, J. F.; Paulsen, I. T.; Fouts, D.; Ravel, J.; Tettelin, H.; Ren, Q.; Read, T.; DeBoy, r. T.; Seshadri, R.; Salzberg, S. L.; Jensen, H. B.; Birkeland, N. K.; Nelson, W. C.; Dodson, R. J.; Grindhaug, S. H.; Holt, I.; Eidhammer, I.; Jonason, I.; Vanaken, S.; Utterback, T.; Feldblyum, T. V.; Fraser, C. M.; Lillehaug, J. R.; Eisen, J. A. *PLoS Biol.* **2004**, *2*, e303.
(74) Kleywegt, G. J. *Acta Crystallogr.* **1996**, *D52*, 842−857.
(75) Solomon, E. I.; Brunold, T. C.; Davis, M. I.; Kemsley, J. N.; Lee, S.-K.; Lehnert, N.; Neese, F.; Skulan, A.; Yang, Y.-S.; Zhou, J. *Chem. Rev.* **2000**, *100*, 235−349.
(76) DeRose, V.; Liu, K. E.; Lippard, S. J.; Hoffman, B. *J. Am. Chem. Soc.* **1993**, *115*, 6440−6441.
(77) Rosenzweig, A. C.; Frederick, C. A.; Lippard, S. J.; Nordlund, P. *Nature* **1993**, *366*, 537−543.
(78) Dauter, Z. *Methods Enzymol.* **2003**, *368*, 288−337.
(79) Carugo, O.; Bordo, D. *Acta Crystallogr.* **1999**, *D55*, 479−483.
(80) Dunietz, B. D.; Beachy, M. D.; Cao, Y.; Whittington, D. A.; Lippard, S. J.; Friesner, R. A. *J. Am. Chem. Soc.* **2000**, *122*, 2828−2839.
(81) Farrar, J. A.; Zumft, W. G.; Thomson, A. J. *Proc. Natl. Acad. Sci. U.S.A.* **1998**, *95*, 9891−9896.
(82) Rasmussen, T.; Berks, B. C.; Sanders-Loehr, J.; Dooley, D. M.; Zumft, W. G.; Thomson, A. J. *Biochemistry* **2000**, *39*, 12753−12756.

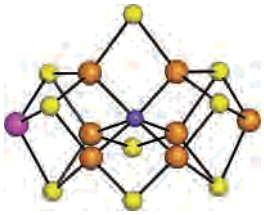

Figure 5. The FeMo-cofactor in the 1.16 Å resolution structure of the *Azotobacter vinelandii* nitrogenase MoFe protein (PDB accession code: 1M1N). Iron ions are shown as orange spheres, the molybdenum ion is shown as a magenta sphere, sulfur atoms are shown as yellow spheres, and the central nitrogen atom is shown as a blue sphere.

repositioning of one of the copper ions, which in turn accounted for some extra electron density previously attributed to a solvent ligand. Another way to confirm the presence of sulfur would have been to collect sulfur anomalous data, a technique currently being developed for phasing.[83]

Another example that underscores the importance of high resolution data in identifying exogenous ligands is the nitrogenase MoFe-protein. Ten years after the first crystal structure,[84] a previously unidentified atom was discovered in the center of the FeMo-cofactor in a 1.16 Å resolution structure[85] (Figure 5). At resolutions lower than 1.55 Å, this atom cannot be detected due to Fourier series termination effects, which produce negative electron density ripples around the iron and sulfur atoms. This ligand has been assigned as nitrogen based on functional considerations and electron spin−echo envelope modulation (ESEEM) data indicating an interaction of the cluster with nitrogen,[86] but oxygen and carbon remain possibilities. The presence of this central ligand has spurred new ENDOR and ESEEM studies[87] as well as density functional calculations.[88,89]

Exogenous ligands are not just important in characterizing resting states of metalloenzymes, but can also provide insight into catalysis. For example, recent structures of dioxygen and nitric oxide bound to the mononuclear copper centers in peptidyl α-amidating monooxygenase[90] and nitrite reductase,[91] respectively, reveal unexpected coordination modes that suggest new mechanistic hypotheses. Similar studies of pMMO would identify the active site and facilitate mechanistic studies.

Conclusions

The examples described here illustrate some of the challenges involved in modeling metal centers in protein crystal structures. Crystallography is an excellent technique for determining metal ion stoichiometry, locating metal ions within a protein fold, and identifying amino acid ligands. Metal ion identity can also be established elegantly using anomalous data collected at different wavelengths. Determining the metal oxidation state is less straightforward and can be facilitated by single crystal spectroscopy. Geometric parameters and the detection of exogenous ligands depend critically on the resolution of the crystal structure. Even in the highest resolution structures, details like protonation of solvent ligands or the identity of light atom ligands can remain ambiguous. When using crystal structures as starting points for mechanistic and computational studies, inorganic chemists should consider these issues. Not every bond or exogenous ligand depicted in a figure can be taken as the ultimate truth: the crystallographer constructs the best model based on the available data and information from spectroscopy and synthetic modeling chemistry. How the crystallographer arrived at the model and draws the line between truth and speculation is usually carefully described in the primary literature and should be taken into account by inorganic chemists. Crystal structures have made major contributions to understanding the function and mechanism of complex metalloenzyme systems, including those highlighted here. With recent technological advances in synchrotron radiation, crystallographic hardware and software, and robotics for protein expression and crystallization, future structures should yield more and more detailed pictures of biological metal centers.

IC0485256

(83) Ramagopal, U. A.; Dauter, M.; Dauter, Z. *Acta Crystallogr.* **2003**, *D59*, 1020−1027.
(84) Kim, J.; Rees, D. C. *Science* **1992**, *257*, 1677−1682.
(85) Einsle, O.; Tezcan, F. A.; Andrade, S. L. A.; Schmid, B.; Yoshida, M.; Howard, J. B.; Rees, D. C. *Science* **2002**, *297*, 1696−1700.
(86) Lee, H.-I.; Thrasher, K. S.; Dean, D. R.; Newton, W. E.; Hoffman, B. M. *Biochemistry* **1998**, *37*, 13370−13378.
(87) Lee, H.-I.; Benton, P. M. C.; Laryukhin, M.; Igarashi, R. Y.; Dean, D. R.; Seefeldt, L. C.; Hoffman, B. M. *J. Am. Chem. Soc.* **2003**, *125*, 5604−5605.
(88) Hinnemann, B.; Nørskov, J. K. *J. Am. Chem. Soc.* **2003**, *125*, 1466−1467.
(89) Hinnemann, B.; Nørskov, J. K. *J. Am. Chem. Soc.* **2004**, *126*, 3920−3927.
(90) Prigge, S. T.; Eipper, B. A.; Mains, R. E.; Amzel, L. M. *Science* **2004**, *304*, 864−867.
(91) Tocheva, E. I.; Rosell, F. I.; Mauk, A. G.; Murphy, M. E. P. *Science* **2004**, *304*, 867−870.